Hindawi
Complexity
Volume 2023, Article ID 6616560, 10 pages
https://doi.org/10.1155/2023/6616560

Research Article

Synchronizability of Discrete Nonlinear Systems: A Master Stability Function Approach

Mohanasubha Ramasamy,[1] **Suresh Kumarasamy**,[2] **Sakthi Kumar Sampathkumar**,[3] **Anitha Karthikeyan**,[4,5] **and Karthikeyan Rajagopal**[2]

[1]*Centre for Nonlinear Systems, Chennai Institute of Technology, Chennai 600069, India*
[2]*Centre for Computational Modeling, Chennai Institute of Technology, Chennai 600069, India*
[3]*Department of Computer Science Engineering, Chennai Institute of Technology, Chennai 600069, India*
[4]*Department of Electronics and Communications Engineering, University Centre for Research and Development, Chandigarh University, Mohali 140413, Punjab, India*
[5]*Department of Electronics and Communication Engineering, Vemu Institute of Technology, Chittoor, Andhra Pradesh 517112, India*

Correspondence should be addressed to Karthikeyan Rajagopal; rkarthiekeyan@gmail.com

Received 2 February 2023; Revised 26 September 2023; Accepted 30 September 2023; Published 20 October 2023

Academic Editor: Carlos Aguilar-Ibanez

In recent times, studies on discrete nonlinear systems received much attention among researchers because of their potential applications in real-world problems. In this study, we conducted an in-depth exploration into the stability of synchronization within discrete nonlinear systems, specifically focusing on the Hindmarsh–Rose map, the Chialvo neuron model, and the Lorenz map. Our methodology revolved around the utilization of the master stability function approach. We systematically examined all conceivable coupling configurations for each model to ascertain the stability of synchronization manifolds. The outcomes underscored that only distinct coupling schemes manifest stable synchronization manifolds, while others do not exhibit this trait. Furthermore, a comprehensive analysis of the master stability function's behavior was performed across a diverse range of coupling strengths (σ) and system parameters. These findings greatly enhance our understanding of network dynamics, as discrete-time dynamical systems adeptly replicate the dynamics of continuous-time models, offering significant reductions in computational complexity.

1. Introduction

Most of the natural processes around are modeled as complex networks. Understanding the collective behaviors of complex networks has attracted researchers from different disciplines over the past decades. In particular, synchronization is one of the vital collective behavior of the complex network of systems which is observed in many areas of research, ranging from neuroscience to social systems [1–8]. Synchronization occurs when the systems in a network behave collectively and have the same dynamics upon the proper coupling strength. Simultaneously, complex networks have been studied by many researchers because of their wide applicability in modeling the dynamics of social networks, epidemics spread such as COVID-19, neuronal networks, prey-predator dynamics, and human brain networks [9]. The synchronization phenomenon has been studied in complex networks in various aspects [10]. For instance, synchronization in complex networks was studied by Arenas et al. in [11]. Coombes and Thul studied the synchrony in networks of coupled nonsmooth dynamical systems [12]. Complex networks with long-range interactions were considered by Rakshit et al., and we found studies on the synchronization in [13]. A detailed study on the network synchronization of various neuron models with the inclusion of electromagnetic flux was investigated in [14]. A detailed study of the synchronization of time-varying networks was also found in [15]. The literature on synchronization is huge, and one may refer to [1, 3, 4, 6, 8, 10, 16–22] and references therein. Recently, several studies have dealt with the synchronization of complex networks with higher-order interactions [23–30].

To investigate the synchronization in complex networks, the master stability function (MSF) is one of the fundamental tools in the nonlinear dynamics literature. We define MSF as the largest transverse Lyapunov exponent of the synchronization manifold. The condition for the occurrence of synchronization is that the value of MSF at certain parameters should be negative. Pecora and Carroll introduced this in the year 1998 to analyze the synchronization in identical networks [31]. The generic behavior of master stability functions in coupled nonlinear dynamical systems was studied in [32]. The MSF of stochastically coupled chaotic maps was studied by Porfiri [33]. In the multivariable coupled oscillators, the synchronization stability has been analyzed using MSF formalism in [34]. Later, the research on the MSF for synchronization stability became a vibrant topic and extended to complex networks with different topologies and structures. For more details, one can refer to [23, 35–39].

In general, the systems/networks are modeled as either continuous-time or discrete-time dynamical systems to understand their dynamics. In the present work, we aim to study networks of discrete systems since various real-life problems, such as neurodynamics and population dynamics, can be modeled as discrete dynamical systems. Most of the studies have given attention to the MSF of continuous dynamical systems. Very few studies in the literature have focused on the synchronization of discrete systems by using MSF. Sun and Cao analyzed the complete synchronization of coupled Rulkov neuron networks with the help of MSF [40]. In [41], the authors have investigated the complete synchronization of a coupled chaotic Aihara neuron network with electrical synapses. In this series, we would like to investigate the synchronization stability of networks of three different discrete maps using the MSF formalism. In this work, we study the stability of synchronization in networks of coupled discrete maps. We consider three different maps: the Hindmarsh–Rose map, the Chialvo neuron model, and the Lorenz map. We investigate the stability of synchronization for all possible coupling configurations in each system. We also find that marginally synchronized states can exist in networks of coupled maps. These states are not fully synchronized, but they are still stable. Interestingly, the Lorenz map exhibits multiple zero crossings and is found to belong to the Γ_4 class.

Our study provides a better understanding of the stability of the synchronization manifold of networks of coupled maps. This information is important for understanding the dynamics of complex networks and for designing networks that can be used for applications such as secure communication and distributed computing. Also, understanding the synchronization dynamics of networks of maps is important in the study of complex network theory, as these discrete-time dynamical systems efficiently replicate the dynamics of continuous-time models with reduced computational effort.

The structure of the article is as follows: in Section 2, we present the theory of discrete MSF. The synchronization of the discrete HR neuron model is analyzed in Section 3. In Section 4, we discuss the MSF studies of another network of neurons, namely the discrete Chialvo neuron model. Another important model, namely the Lorenz map and its synchronization stability through MSF, is presented in Section 5. Finally, we give a summary and conclusion in Section 6.

2. Background

A general model of a discrete nonlinear difference equation is given by

$$x(k+1) = F(x(k)). \tag{1}$$

In [32], the authors have proposed a master stability function approach to understand the synchronizability of a network of N coupled oscillators for continuous-time systems. We rewrite the same procedure for discrete-time systems in the following way [42]. With the coupling matrix C (Laplacian matrix) and the coupling function $H(x)$, the coupled systems of N maps can be modeled as follows:

$$x_i(k+1) = F(x_i(k)) - \rho \sum_{m=1}^{N} C_{\mathrm{im}} H(x_m(k)), \quad i = 1, 2, \cdots, N, \tag{2}$$

where $x_i(k)$ denotes n-dimensional state vector of the i^{th} system at discrete-time k, $(= 0, 1, 2, \cdots)$.

If the connection exists between the nodes i and m, then the coupling matrix C_{im} has the value 1, otherwise 0. The Laplacian matrix should be $\sum_{m-1}^{N} C_{\mathrm{im}} = 0$ for any value of m in order to have the solution of equation (2) as the synchronized states $x_1(k) = x_2(k) = \cdots = x_N(k) = s(k)$. Here, $s(k)$ is the synchronized solution of the isolated system (1) (solution means a fixed point, a periodic orbit, or even a chaotic orbit of the uncoupled system).

$$x_i(k) = s_i(k) + y_i(k). \tag{3}$$

From the master stability equation,

$$y_l(k+1) = \left(\mathrm{DF}(s(k)) - \rho \sum_{m=1}^{N} C_{\mathrm{lm}} \mathrm{DH}(s(k)) \right) y_l(k). \tag{4}$$

We analyze the stability of equation (2) at the synchronized state $s(k)$. Here, $y_l(k)$ is the variation about the synchronized state $s(k)$. The terms $\mathrm{DF}(s(k))$ and $\mathrm{DH}(s(k))$ define the Jacobian matrix for the velocity functions $F(x(k))$ and coupling function $H(x(k))$ evaluated on the synchronization manifold $s(k)$. Significance of velocity function $F(x(k))$ and coupling function $H(x(k))$ can be found in [32]. In [35], the authors have derived a new method by using a block diagonalized coupling function with the help of the matrix Q, which is constructed from the eigenvectors of the Laplacian matrix C, and the difference equation in (4) is changed to

$$\begin{aligned} z(k) &= Q^{-1} y(k), \\ z_l(k+1) &= (\mathrm{DF}(s(k)) - \sigma \mathrm{DH}(s(k))) z_l(k). \end{aligned} \tag{5}$$

where σ is the coupling strength and is denoted by $\rho\lambda_l$ where λ_l corresponds to the eigenvalue of the Laplacian matrix C_{lm}. The well-known Lyapunov and Floquet methods of MSF calculations need complex computations and longer simulation time; hence, as in [35], the error-based method is used. The coupled map network model defined by (5) is numerically solved, and the state variable (z) should be close to zero or unbounded, and the logarithm of these ends is used as the master stability function (MSF) of the coupled discrete network. The master stability function (ψ) is calculated from the largest Lyapunov exponent from the equation (5). If the MSF (ψ) is negative, then the stability of the synchronized state can be determined by small disturbance, which eventually will diminish exponentially so that the synchronous solution is stable. The synchronous solution becomes unstable, and the largest Lyapunov exponent is positive. This is because a tiny perturbation from the synchronous state will lead to trajectories that diverge from the state. As a function of coupling strength, the MSF may cross zero several times. Depending on the number of crossings, the class or the classification of MSF is defined. Class Γ_0 is characterized by the absence of any finite zero crossings and is always in a positive state. This means that the network never allows synchronization to occur. Similarly, class Γ_t exhibits a single finite zero crossing, signifying that once the network achieves synchronization, and it remains in that synchronized state. On the other hand, class Γ_2 displays two finite zero crossings. In this class, there exists a finite range of coupling parameters where network synchronization can occur. However, as soon as the MSF becomes positive, the network desynchronizes. Likewise, classes Γ_3 and Γ_4 depend on the number of times MSF crosses the zero axis. To show the effectiveness of the proposed discrete MSF, we have chosen the discrete HR model [43, 44], the discrete Chialvo model [45], and the Lorenz map [46]. We use MATLAB to solve the network of oscillators with $k = 20000$ and after removing enough transient.

3. Case A: Discrete Hindmarsh–Rose Model (HR)

The three-dimensional HR map proposed in [44] is defined by the following difference equations:

$$\begin{aligned} x(k+1) &= x(k) + \delta\left(y(k) - ax(k)^3 + bx(k)^2 - z(k) + I\right), \\ y(k+1) &= y(k) + \delta\left(c - dx(k)^2 - y(k)\right), \\ z(k+1) &= z(k) + \delta\left(r\left(s\left(x(k) + 1.6\right) - z(k)\right)\right). \end{aligned} \tag{6}$$

Here, $x(k)$, $y(k)$, and $z(k)$ denote the system variables, and we have used the parameters as defined in [44]. The parameters δ and k are defined as integration step size and discrete-time $(k = 1, 2, 3, \cdots)$, respectively. The other system parameters take the following values: $a = 1, b = 3, c = 1, d = 5, s = 4, r = 0.006$, and $I = 3.3$. Studies on various aspects of the Hindmarsh–Rose model in the continuous case are discussed in [28, 47–49]. Synchronization stability of the continuous-time Hindmarsh–Rose has been reported for various choices of coupling schemes [32]. However, a detailed understanding of the stability of synchronization of the discrete-time Hindmarsh–Rose model is not fully reported in the literature. In order to understand the stability of the synchronization, we write the Jacobian matrix of the discrete HR map (6) as follows:

$$J = \begin{bmatrix} 1 + \delta\left(-3ax^2(k) + 2bx(k)\right) & \delta & -\delta \\ -2\delta \mathrm{d}x(k) & 1-\delta & 0 \\ \delta rs & 0 & 1-\delta r \end{bmatrix}. \tag{7}$$

By using the error-based MSF model (5) and the Jacobian matrix (7), the new variational equation of the coupled discrete HR model is derived as follows:

$$\begin{bmatrix} z_1(k+1) \\ z_2(k+1) \\ z_3(k+1) \end{bmatrix} = \begin{bmatrix} 1 + \delta m - \sigma & \delta & -\delta \\ -2\delta \mathrm{d}x(k) & 1-\delta & 0 \\ \delta rs & 0 & 1-\delta r \end{bmatrix} \begin{bmatrix} z_1(k) \\ z_2(k) \\ z_3(k) \end{bmatrix}, \tag{8}$$

where $m = (-3ax^2(k) + 2bx(k))$. The above model is a representation of $x - x$ coupling scheme. Depending on the variables coupled, the model (8) has nine different coupling matrices whose master stability function plots are shown in Figure 1. In the $x - x$ coupling scheme, the MSF crosses zero and enters into synchronization region at $\sigma = 0.04311$ which is marked in blue color in Figure 1(a). The discrete HR neuron model shows a longer range of coupling strength in the synchronized region. Further increasing the coupling strength, the MSF crosses zero to the positive region at the coupling strength $\sigma = 2.619$ which is marked in red color in the same figure. The $x - x$ coupling scheme is categorized into Γ_2 with two finite crossing points. The MSF for the coupling scheme $x - y$ is presented in Figure 1(b). From this figure, we observed the MSF crosses zero and entered the synchronized region at the value of $\sigma = 0.08919$. It remains in the synchronized regime only for a short range of coupling strength σ up to $\sigma = 0.1225$. When σ is increased beyond 0.1225, the MSF again crosses zero to the positive region. Though the $x - y$ coupling has a short parameter range of synchronization, this coupling scheme also falls under the category of Γ_2 with two finite crossing points. As far as the $x - z$ coupling scheme is concerned, the MSF reaches zero at the value of $\sigma = 0.03117$, and it entered back to the positive region without going further into the negative region. Here, the HR neurons are marginally synchronized at the σ has the value $\sigma = 0.03117$. In the case of marginally synchronization, the network has some degree of synchronization among the components, and it is not strong enough to ensure complete or perfect synchronization. This is marked in green color in Figure 1(c).

Likewise, when a couple of other possible pairs of variables, MSF crosses zero value two times when we opted for the $y - y$ coupling scheme. At $\sigma = 0.03148$ (blue color), the MSF moves to a negative region and the synchronization

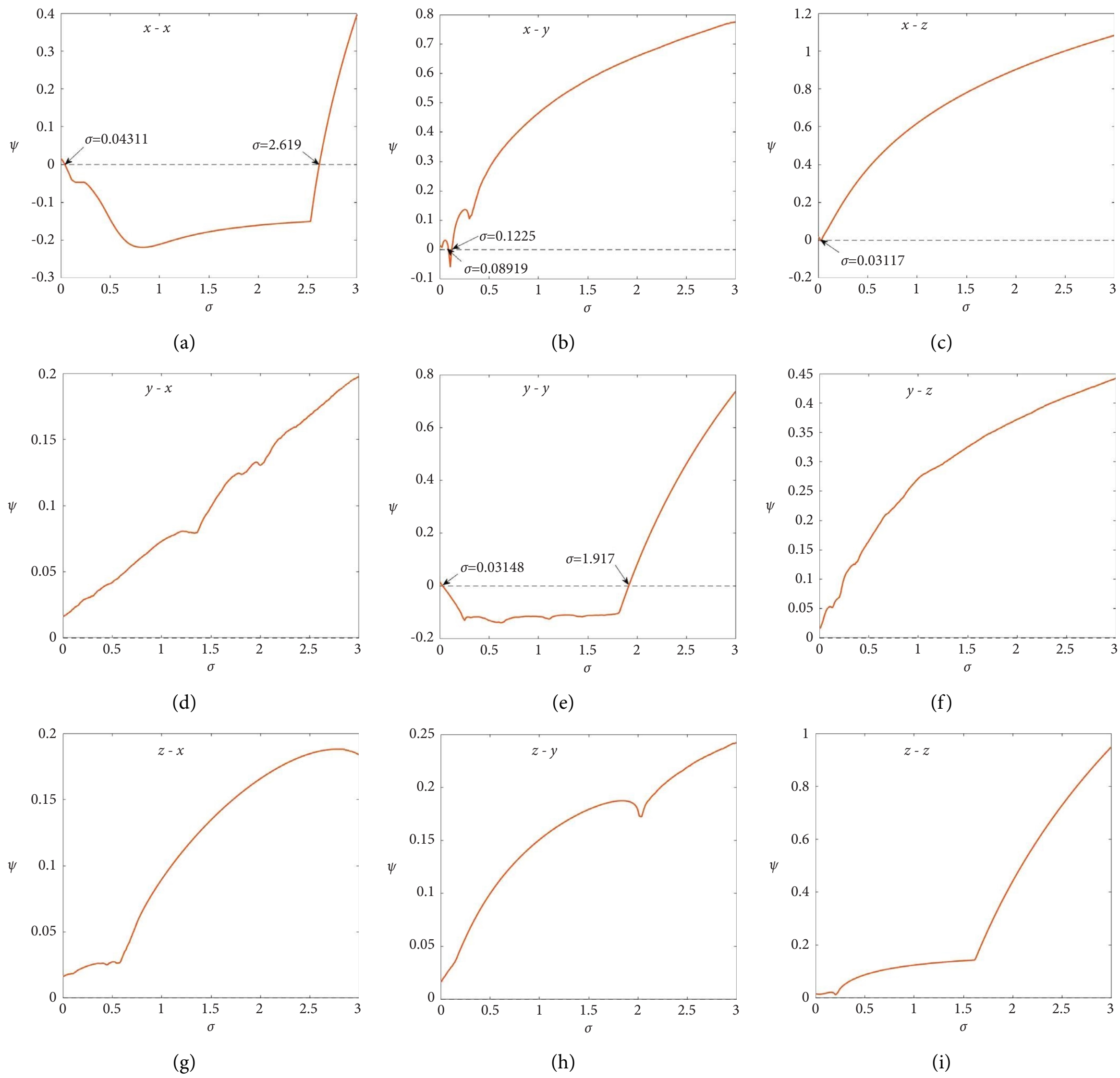

Figure 1: MSF of the nine different coupling schemes for discrete HR neuron model (6). (a–c) depict ψ over σ for the coupling schemes $x-x$, $x-y$, and $x-z$, respectively. Likewise, for the coupling schemes $y-x$, $y-y$, and $y-z$, ψ versus σ are plotted as $2D$ plots in (d–f). The response of ψ versus σ for the other coupling schemes $z-x$, $z-y$, and $z-z$ is displayed in (g–i).

manifold of the coupled systems is stable while MSF moves back to the positive value for σ greater than 1.917 (red color), and hence, the synchronization manifold is unstable which is shown in Figure 1(e). The $y-y$ coupling scheme falls under the category of Γ_2 with two finite crossing points. The rest of the combinations of the coupling schemes discussed in Figures 1(d) and 1(f)–1(i) show that the synchronization manifold of the coupled discrete HR neurons remains unstable for any given value of the σ. All these coupling schemes come under the category Γ_0 since there are no finite crossing points.

Similar to the parameter σ, the parameter I shows a significant effect on the stability of the synchronization manifold. To check the effect of I, we have plotted Figure 2, which shows the effect of MSF versus the external current I and the coupling strength σ for the coupling scheme $x-x$. Colors in the image plot clearly show how the regime of synchronization and unsynchronization stability changes with respect to the parameters σ and I. In particular, the sky blue color regime indicates the synchronization of HR neurons, and green, yellow, and pink colors indicate the unsynchronized part of the HR neurons.

Next, we would like to analyze another neuron model, namely the discrete Chialvo neuron model.

4. Discrete Chialvo Neuron Model

The mathematical model of the Chialvo neuron [50] is defined as follows:

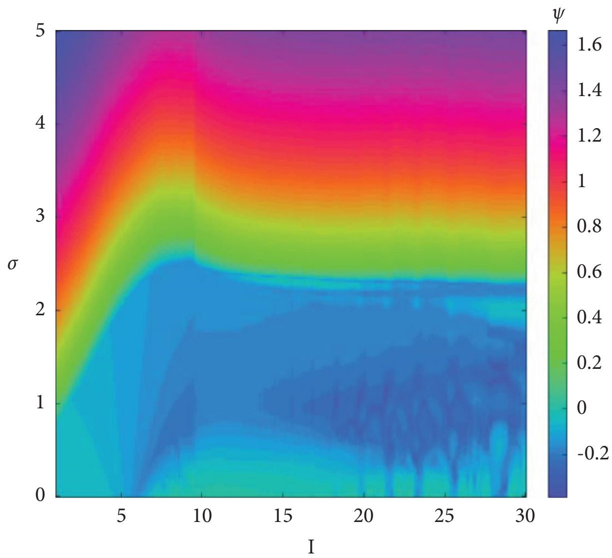

FIGURE 2: The effect of MSF with the coupling strength σ and the external current I.

$$\begin{aligned} x(k+1) &= x(k)^2 e^{(y(k)-x(k))} + k_1 + p x(k)\tanh(z(k)), \\ y(k+1) &= a y(k) - b x(k) + c, \\ z(k+1) &= z(k) + \varepsilon x(k). \end{aligned} \tag{9}$$

Variables $x(k)$, $y(k)$, and $z(k)$ define the activation variable, recovery variable, and magnetic flux across the neuron membrane, respectively. Constant bias is defined by the parameter k_1, and it has the value $k_1 = 0.03$. The dimensionless parameters used in (9) are defined as $a = 0.88, b = 0.18, c = 0.28, \varepsilon = 0.01, p = 0.01$. For more details, studies related to Chialvo neurons are found in [51, 52]. To the best of our knowledge, the stability of the synchronization for the discrete-time Chialvo neurons has not been reported in the literature. Studies have been conducted to understand the synchronization dynamics of the Chialvo neurons not on the stability of synchronization [53]. We write the Jacobian matrix of the model (9) as follows:

$$J = \begin{bmatrix} f_1 & f_2 & f_3 \\ -b & a & 0 \\ \varepsilon & 0 & 1 \end{bmatrix}, \tag{10}$$

where the expressions f_1, f_2, and f_3 take the form

$$\begin{aligned} f_1 = &-x^2(k)e^{y(k)-x(k)} + 2x(k)e^{y(k)-x(k)} \\ &+ p\tanh(z(k)), \end{aligned} \tag{11}$$

$$f_2 = x^2(k)e^{y(k)-x(k)}, \tag{12}$$

$$f_3 = p x(k)\left(1 - \tanh z(k)^2\right). \tag{13}$$

An error-based equation can be derived using (9) and (10), as well as the new variational equation of the Chialvo neuron model, which is derived for the $x-x$ coupling as follows:

$$\begin{bmatrix} z_1(k+1) \\ z_2(k+1) \\ z_3(k+1) \end{bmatrix} = \begin{bmatrix} f_1-\sigma & f_2 & f_3 \\ -b & a & 0 \\ \varepsilon & 0 & 1 \end{bmatrix} \begin{bmatrix} z_1(k) \\ z_2(k) \\ z_3(k) \end{bmatrix}, \tag{14}$$

where σ is the coupling term for the $x-x$ coupling configuration. For the numerical analysis, we considered all nine possible combinations of the coupling schemes as we did in the previous case. From Figure 3, we observe that the stability of the synchronization manifold of coupled Chialvo neurons map happens only for two coupling schemes, namely $x-x$ and $y-y$. Both the coupling schemes belong to the class Γ_2 with two finite crossing points. The synchronization manifold stability sustains a wide range of coupling strengths σ. In the first-coupling scheme $(x-x)$, the MSF reaches zero at $\sigma = 0.1116$ (blue color) and enters into the synchronized region. The MSF sustains in the zero for a wide range from $\sigma = 0.1116$ to $\sigma = 2.043$. As we increase coupling strength $\sigma > 2.043$, it moves to a positive (unsynchronized) region (red color) which is given in Figure 3(a). Likewise, for the $y-y$ coupling scheme, as we increase the coupling strength, the MSF becomes zero from the positive region at $\sigma = 0.09985$ (blue color). The MSF remains zero for a wide range of coupling strength and enters into an unsynchronized region at the σ value 1.882 (red color) which is shown in Figure 3(e). For $x-y$ coupling, the value of ψ reaches zero at $\sigma = 0.0241$, and the Chialvo neurons are marginally synchronized which is marked as green color in Figure 3(b). Other coupling combinations such as $x-z$, $y-x$, $y-z$, and $z-z$ show positive MSF value (ψ) of the coupling parameter range from 0 to 3. Some of the coupling combinations, such as $z-x$ and $z-y$, show almost no change in the MSF as we change the coupling parameter σ. It means that the coupling parameter does not influence the stability of the synchronization manifold. All the other coupling schemes $(x-z$, $y-x$, $y-z$, and $z-z)$ show no stable synchronization manifold so they belong to class Γ_0 with no finite crossing point. The dashed line shows the zero value of the MSF, which is the separation of synchronized and unsynchronized regimes.

To show the stability of the synchronization manifold of the system with various parameter regimes, we have plotted the MSF as a function of the parameter k_1 and coupling strength σ. The image plot shows the effect of MSF versus the parameters k_1 and σ for the $x-x$ coupling scheme is presented in Figure 4. From the image plot, we have seen that the coupling strength ranges from 0 to 5, and the parameter k_1 ranges from 0 to 0.2, and the system remains in the unsynchronized region.

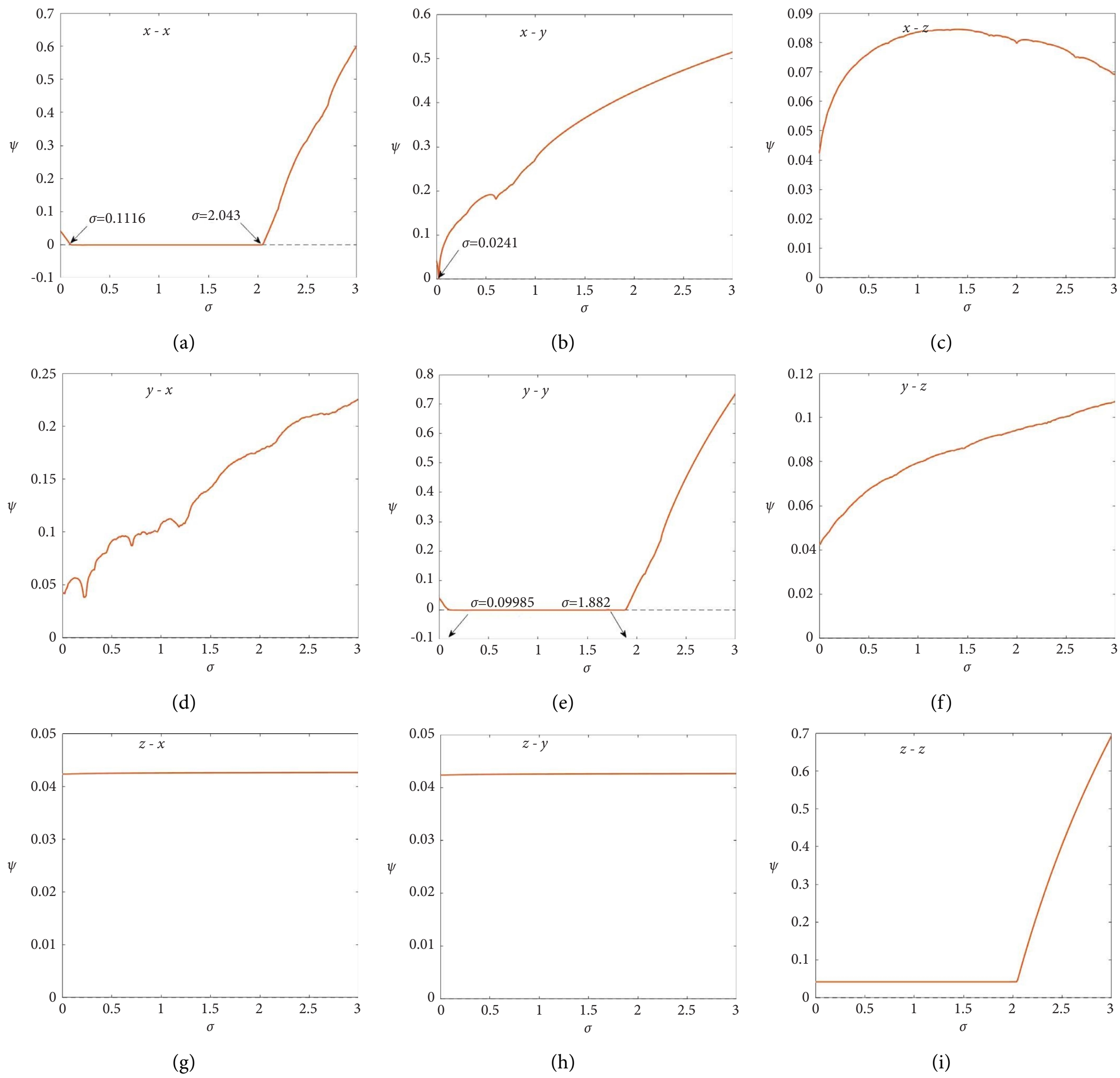

Figure 3: The response of MSF versus coupling strength σ for different coupling schemes is discussed here. For the coupling schemes $x - x$, $x - y$, and $x - z$, the effect of MSF versus the coupling strength σ is depicted in (a–c). Likewise, for the coupling schemes $y - x$, $y - y$, and $y - z$, ψ over σ is presented in (d–f). The outcome of ψ versus σ is shown as $2D$ plots (g–i) for the coupling schemes $z - x$, $z - y$, and $z - z$.

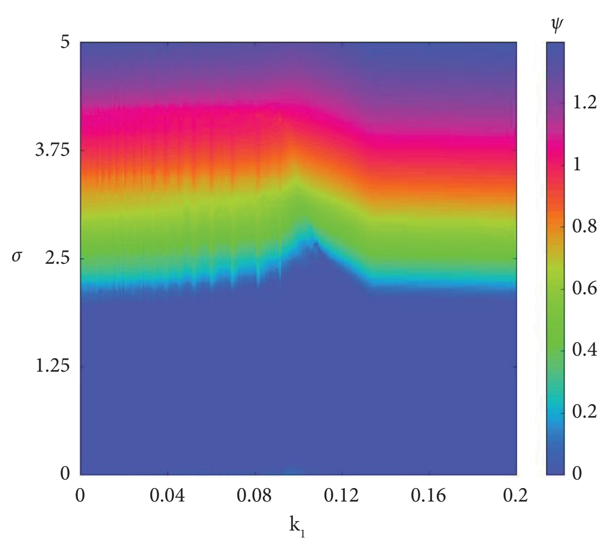

Figure 4: Image plot for the MSF analysis ψ versus the system parameter k_1 and the coupling strength σ.

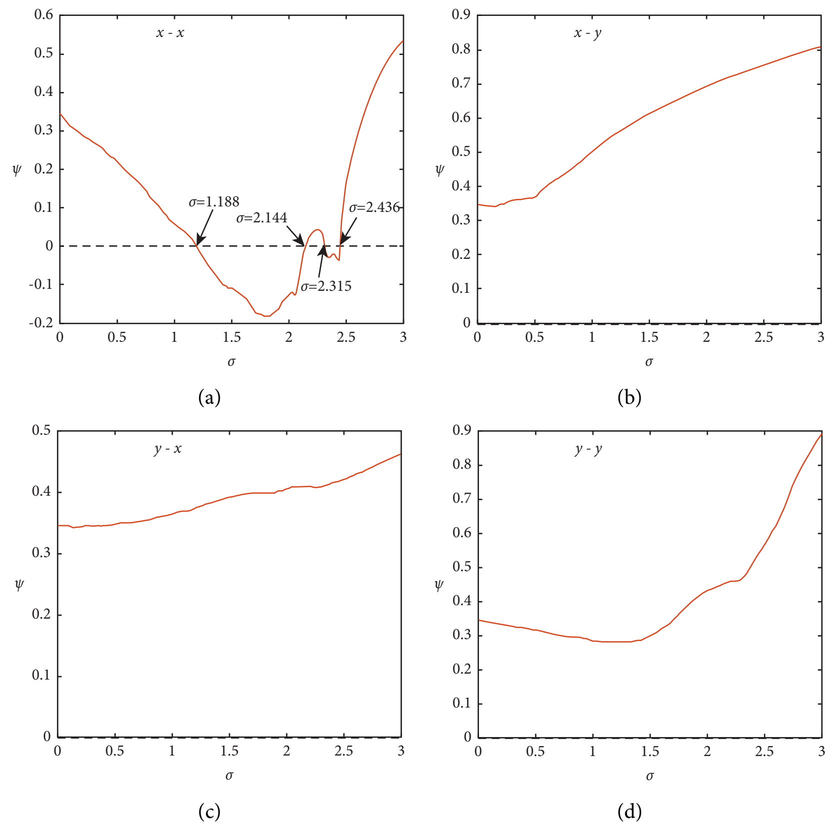

FIGURE 5: (a, b) MSF analysis for the coupling schemes $x-x$ and $x-y$ of Lorenz map. Likewise, for the other two coupling schemes $y-x$ and $y-y$, ψ versus σ are plotted in (c, d).

5. Lorenz Map

The mathematical model for a Lorenz map can be written as [46] follows:

$$\begin{aligned} x(k+1) &= (1+ab)x(k) - bx(k)y(k), \\ y(k+1) &= (1-b)y(k) + bx(k)^2. \end{aligned} \tag{15}$$

The system parameters are denoted as a and b. Followed by the introduction of the Lorenz map in [46], its synchronization dynamics and stability of the synchronization have not been studied in the literature. The Jacobian matrix associated with (15) can be written as follows:

$$J = \begin{bmatrix} 1+ab-by(k) & -bx(k) \\ 2bx(k) & 1-b \end{bmatrix}. \tag{16}$$

We derive the error-based equation by using (15) and (16), and it takes the following form:

$$\begin{bmatrix} z_1(k+1) \\ z_2(k+1) \end{bmatrix} = \begin{bmatrix} 1+ab-by(k)-\sigma & -bx(k) \\ 2bx(k) & 1-b \end{bmatrix} \begin{bmatrix} z_1(k) \\ z_2(k) \end{bmatrix}, \tag{17}$$

where σ represents the coupling strength. The above representation is given for the $x-x$ coupling scheme.

For the $x-x$ coupling, initially, the MSF becomes stable at $\sigma = 1.188$, while increasing the coupling parameter, the synchronization stability breaks, and the MSF becomes positive (synchronization manifold is unstable) at $\sigma = 2.144$. The unstable synchronization manifold becomes stable again $\sigma = 2.315$. However, the synchronization stability breaks again when we increase the coupling strength to $\sigma = 2.436$. We plotted all these transitions of MSF in Figure 5(a). As we can see that the zero crossing happens four times, it comes under the class of Γ_4. When the MSF crosses zero for the first time at $\sigma = 1.188$, the synchronization stays for the longer range of coupling strength up to σ and reaches the value $\sigma = 2.144$. Once the MSF enters the positive region, it remains there for only a short range of σ value, and it approaches the negative region at $\sigma = 2.315$. Likewise, after a short range of σ value, the MSF crosses zero at $\sigma = 2.436$ and becomes unstable (positive value). Figure 5, we observed that for all other types of coupling such as $x-y$, $y-y$, and $y-x$, the MSF of the systems becomes unstable. The synchronization stability of the map does not occur, that is, MSF does not cross the zero value, and hence, all these coupling schemes belong to class Γ_0 since there is no zero crossing.

To show the behavior of the MSF over a wide range of parameters, we have plotted MSF versus coupling strength σ and the system parameters a and b which are shown in Figure 6. Figure 6(a) depicts the MSF of the coupled map as a function of coupling strength σ and the system parameter b for the $x-x$ coupling scheme. We can see an island of the regime of negative values of MSF which is marked in blue

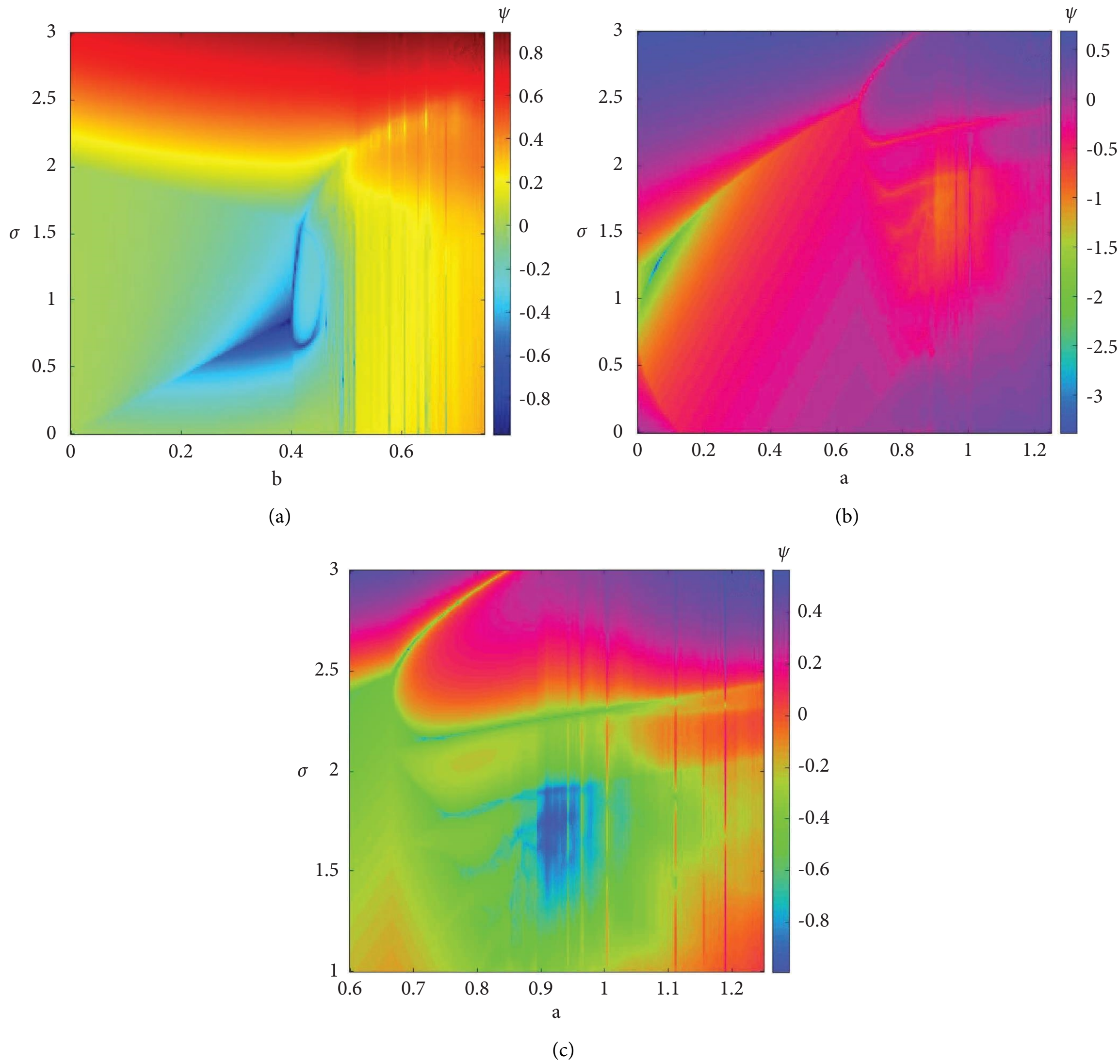

Figure 6: Image plot of the MSF (ψ) as a function of (a) coupling strength σ and the system parameter b and (b) coupling strength σ and the system parameter a. An enlarged view of (b) is displayed in (c) for the range $a \in (0.6, 1.3)$ and $\sigma \in (1, 3)$.

color, where the system has synchronization stability. The unsynchronized regimes are marked with yellow and red colors. The image plot of MSF versus the coupling strength σ and the other system parameter a for the range 0 to 1.25 is plotted in Figure 6(b). The blue, green, yellow, and green regions indicate the synchronized state whereas pink and pinkish blue indicate the unsynchronized region. The enlarged view of Figure 6(b) for the range of system parameter a from 0.6 to 1.25 is shown in Figure 6(c). The plot of MSF between the parameters σ and a shows a wide range of stable synchronization manifolds.

6. Conclusion

In this study, we analyzed the stability of synchronization in discrete complex networks. Specifically, we considered three different types of discrete networks: the Hindmarsh–Rose neuron model, the Chialvo neuron model, and the Lorenz map. For the HR neuron model, we examined nine different coupling configurations to analyze the synchronization stability among the discrete neurons. Our analysis revealed that discrete HR neurons exhibited synchrony in only four coupling schemes. Similarly, for the Chialvo neuron model, we observed synchronization occurring in three specific coupling schemes. In the case of the Lorenz map, synchronization stability was found exclusively in the $x - x$ coupling scheme. We also presented image plots for all the considered discrete nonlinear models, providing a visual representation of their dynamics. Across all three maps, we observed that the $x - x$ coupling schemes demonstrated a longer range of synchronization stability compared to other coupling schemes. To investigate synchronization stability, we utilized a variety of analytical and numerical methods, including linear stability analysis and numerical simulations.

Our findings indicated that the stability of synchronization depends on several factors, such as the type of map, the strength of coupling, and the network topology. Furthermore, we discovered the existence of marginally synchronized states in networks of coupled maps. Although these states are not fully synchronized, they remain stable. These results contribute valuable insights into the stability of synchronization in networks of coupled maps. Understanding these dynamics is crucial for designing networks applicable in fields such as secure communication and distributed computing. Given the emergence of new dynamics, such as marginal synchronization and multiple zero crossings of MSF (master stability function), it would be intriguing to explore these behaviors in fractional-order discrete complex networks. In particular, investigating the impact of fractional order on synchronization stability using MSF analysis holds promise for further exploration.

Data Availability

The data that support the findings of this study are available from the corresponding author upon reasonable request.

Conflicts of Interest

The authors declare that they have no conflicts of interest.

Acknowledgments

This work was partially funded by the Center for Computational Biology, Chennai Institute of Technology, India, vide funding number CIT/CCM/2022/RD/005.

References

[1] A. Pikovsky, M. Rosenblum, and J. Kurths, *Synchronization: A Universal Concept in Nonlinear Sciences*, Cambridge University Press, Cambridge, UK, 2003.

[2] A. Barrat, M. Barthelemy, and A. Vespignani, *Dynamical Processes on Complex Networks*, Cambridge University Press, Cambridge, UK, 2008.

[3] J. D. J. Rubio, "Stability analysis of the modified levenberg–marquardt algorithm for the artificial neural network training," *IEEE Transactions on Neural Networks and Learning Systems*, vol. 32, no. 8, pp. 3510–3524, 2021.

[4] J. D. J. Rubio, "Bat algorithm based control to decrease the control energy consumption and modified bat algorithm based control to increase the trajectory tracking accuracy in robots," *Neural Networks*, vol. 161, pp. 437–448, 2023.

[5] H. S. Chiang, M. Y. Chen, and Y. J. Huang, "Wavelet-based EEG processing for epilepsy detection using fuzzy entropy and associative petri net," *IEEE Access*, vol. 7, pp. 103255–103262, 2019.

[6] J. D. J. Rubio, D. Garcia, H. Sossa, I. Garcia, A. Zacarias, and D. Mujica-Vargas, "Energy processes prediction by a convolutional radial basis function network," *Energy*, vol. 284, Article ID 128470, 2023.

[7] D. M. Vargas, "Superpixels extraction by an Intuitionistic fuzzy clustering algorithm," *Journal of Applied Research and Technology*, vol. 19, no. 2, pp. 140–152, 2021.

[8] A. López-González, J. Meda Campaña, E. Hernández Martínez, and P. P. Contro, "Multi robot distance based formation using Parallel Genetic Algorithm," *Applied Soft Computing*, vol. 86, Article ID 105929, 2020.

[9] E. Estrada, *The Structure of Complex Networks: Theory and Applications*, Oxford University Press, Oxford, UK, 2012.

[10] S. Boccaletti, A. N. Pisarchik, C. I. Del Genio, and A. Amann, *Synchronization: From Coupled Systems to Complex Networks*, Cambridge University Press, Cambridge, UK, 2018.

[11] A. Arenas, A. Díaz-Guilera, J. Kurths, Y. Moreno, and C. Zhou, "Synchronization in complex networks," *Physics Reports*, vol. 469, no. 3, pp. 93–153, 2008.

[12] S. Coombes and R. Thul, "Synchrony in networks of coupled non-smooth dynamical systems: extending the master stability function," *European Journal of Applied Mathematics*, vol. 27, no. 6, pp. 904–922, 2016.

[13] S. Rakshit, S. Majhi, and D. Ghosh, "Synchronization in complex networks with long-range interactions," *Journal of Physics A: Mathematical and Theoretical*, vol. 53, no. 15, Article ID 154002, 2020.

[14] K. Rajagopal, S. Jafari, A. Karthikeyan, and A. Srinivasan, "Effect of magnetic induction on the synchronizability of coupled neuron network," *Chaos*, vol. 31, no. 8, Article ID 83115, 2021.

[15] D. Ghosh, M. Frasca, A. Rizzo et al., "The synchronized dynamics of time-varying networks," *Physics Reports*, vol. 949, pp. 1–63, 2022.

[16] S. Majhi and D. Ghosh, "Synchronization of moving oscillators in three dimensional space," *Chaos*, vol. 27, no. 5, Article ID 53115, 2017.

[17] C. W. Wu, *Synchronization in Complex Networks of Nonlinear Dynamical Systems*, World Scientific, Singapore, 2007.

[18] P. S. Swathy, S. Sabarathinam, K. Suresh, and K. Thamilmaran, "Chaos synchronization and transmission of information in coupled SC-CNN-based canonical Chua's circuit," *Nonlinear Dynamics*, vol. 78, no. 2, pp. 1033–1047, 2014.

[19] V. Varshney, S. Kumarasamy, A. Mishra, B. Biswal, and A. Prasad, "Traveling of extreme events in network of counter-rotating nonlinear oscillators," *Chaos*, vol. 31, no. 9, Article ID 93136, 2021.

[20] H. S. Chiang, M. Y. Chen, and Y. J. Huang, "Wavelet-based EEG processing for epilepsy detection using fuzzy entropy and associative petri net," *IEEE Access*, vol. 7, pp. 103255–103262, 2019.

[21] D. M. Vargas, "Superpixels extraction by an Intuitionistic fuzzy clustering algorithm," *Journal of Applied Research and Technology*, vol. 19, no. 2, pp. 140–152, 2021.

[22] S. Kumarasamy, A. Srinivasan, M. Ramasamy, and K. Rajagopal, "Strange nonchaotic dynamics in a discrete FitzHugh–Nagumo neuron model with sigmoidal recovery variable," *Chaos*, vol. 32, no. 7, Article ID 73106, 2022.

[23] L. V. Gambuzza, F. Di Patti, L. Gallo et al., "Stability of synchronization in simplicial complexes," *Nature Communications*, vol. 12, no. 1, pp. 1255–1313, 2021.

[24] M. S. Anwar and D. Ghosh, "Intralayer and interlayer synchronization in multiplex network with higher-order interactions," *Chaos*, vol. 32, no. 3, Article ID 33125, 2022.

[25] P. S. Skardal and A. Arenas, "Higher order interactions in complex networks of phase oscillators promote abrupt synchronization switching," *Communications Physics*, vol. 3, no. 1, pp. 218–226, 2020.

[26] Y. Zhang, M. Lucas, and F. Battiston, "Do higher-order interactions promote synchronization?" 2022, https://www.researchgate.net/publication/359079670_Do_higher-order_interactions_promote_synchronization.

[27] F. Battiston, E. Amico, A. Barrat et al., "The physics of higher-order interactions in complex systems," *Nature Physics*, vol. 17, no. 10, pp. 1093–1098, 2021.
[28] F. Parastesh, M. Mehrabbeik, K. Rajagopal, S. Jafari, and M. Perc, "Synchronization in Hindmarsh–Rose neurons subject to higher-order interactions," *Chaos*, vol. 32, no. 1, Article ID 13125, 2022.
[29] F. Battiston, G. Cencetti, I. Iacopini et al., "Networks beyond pairwise interactions: structure and dynamics," *Physics Reports*, vol. 874, pp. 1–92, 2020.
[30] M. Ramasamy, S. Devarajan, S. Kumarasamy, and K. Rajagopal, "Effect of higher-order interactions on synchronization of neuron models with electromagnetic induction," *Applied Mathematics and Computation*, vol. 434, Article ID 127447, 2022.
[31] L. M. Pecora and T. L. Carroll, "Master stability functions for synchronized coupled systems," *Physical Review Letters*, vol. 80, no. 10, pp. 2109–2112, 1998.
[32] L. Huang, Q. Chen, Y. C. Lai, and L. M. Pecora, "Generic behavior of master-stability functions in coupled nonlinear dynamical systems," *Physical Review A*, vol. 80, no. 3, Article ID 36204, 2009.
[33] M. Porfiri, "A master stability function for stochastically coupled chaotic maps," *EPL*, vol. 96, no. 4, Article ID 40014, 2011.
[34] R. Sevilla-Escoboza, R. Gutierrez, G. Huerta-Cuellar et al., "Enhancing the stability of the synchronization of multivariable coupled oscillators," *Physical Review A*, vol. 92, no. 3, Article ID 32804, 2015.
[35] S. Panahi and S. Jafari, "A fast technique for calculating master stability function," *International Journal of Modern Physics B*, vol. 34, no. 5, Article ID 2050024, 2020.
[36] F. Sorrentino and M. Porfiri, "Analysis of parameter mismatches in the master stability function for network synchronization," *EPL*, vol. 93, no. 5, Article ID 50002, 2011.
[37] J. Ramadoss, K. Rajagopal, H. Natiq, and I. Hussain, "The linearity of the master stability function," *Europhysics Letters*, vol. 139, no. 1, Article ID 12002, 2022.
[38] L. Tang, X. Wu, J. Lü, J. A. Lu, and R. M. D'Souza, "Master stability functions for complete, intralayer, and interlayer synchronization in multiplex networks of coupled Rössler oscillators," *Physical Review A*, vol. 99, no. 1, Article ID 12304, 2019.
[39] L. Gallo, R. Muolo, L. V. Gambuzza, V. Latora, M. Frasca, and T. Carletti, "Synchronization induced by directed higher-order interactions," *Communications Physics*, vol. 5, no. 1, p. 263, 2022.
[40] H. Sun and H. Cao, "Complete synchronization of coupled Rulkov neuron networks," *Nonlinear Dynamics*, vol. 84, no. 4, pp. 2423–2434, 2016.
[41] S. Li, Y. He, and H. Cao, "Necessary conditions for complete synchronization of a coupled chaotic Aihara neuron network with electrical synapses," *International Journal of Bifurcation and Chaos*, vol. 29, no. 5, Article ID 1950063, 2019.
[42] Y. Zhang and S. H. Strogatz, "Designing temporal networks that synchronize under resource constraints," *Nature Communications*, vol. 12, no. 1, p. 3273, 2021.
[43] J. L. Hindmarsh and R. M. Rose, "A model of neuronal bursting using three coupled first order differential equations," *Proceedings of Royal Society B*, vol. 221, pp. 87–102, 1984.
[44] C. C. Felicio and P. C. Rech, "Arnold tongues and the Devil's Staircase in a discrete-time Hindmarsh–Rose neuron model," *Physics Letters A*, vol. 379, no. 43-44, pp. 2845–2847, 2015.
[45] D. R. Chialvo, "Generic excitable dynamics on a two-dimensional map," *Chaos, Solitons & Fractals*, vol. 5, no. 3-4, pp. 461–479, 1995.
[46] L. Gardini and W. Tikjha, "The Lorenz model in discrete time," *Journal of Difference Equations and Applications*, vol. 28, no. 10, pp. 1308–1333, 2022.
[47] A. Bandyopadhyay and S. Kar, "Impact of network structure on synchronization of Hindmarsh–Rose neurons coupled in structured network," *Applied Mathematics and Computation*, vol. 333, pp. 194–212, 2018.
[48] D. Chen, J. Li, W. Zeng, and J. He, "Topology identification and dynamical pattern recognition for Hindmarsh–Rose neuron model via deterministic learning," *Cognitive Neurodynamics*, vol. 17, no. 1, pp. 203–220, 2023.
[49] M. Sa and M. Ah, "Synchronization of hindmarsh-rose neurons," *Neural Networks*, vol. 123, pp. 372–380, 2020.
[50] F. Wang and H. Cao, "Mode locking and quasiperiodicity in a discrete-time Chialvo neuron model," *Communications in Nonlinear Science and Numerical Simulation*, vol. 56, pp. 481–489, 2018.
[51] C. Shang, S. He, K. Rajagopal, H. Wang, and K. Sun, "Dynamics and chimera state in a neural network with discrete memristor coupling," *The European Physical Journal- Special Topics*, vol. 231, no. 22-23, pp. 4065–4076, 2022.
[52] I. Bashkirtseva, L. Ryashko, J. Used, J. M. Seoane, and M. A. Sanjuán, "Noise-induced complex dynamics and synchronization in the map-based Chialvo neuron model," *Communications in Nonlinear Science and Numerical Simulation*, vol. 116, Article ID 106867, 2023.
[53] G. Vivekanandhan, H. Natiq, Y. Merrikhi, K. Rajagopal, and S. Jafari, "Dynamical analysis and synchronization of a new memristive Chialvo neuron model," *Electronics*, vol. 12, no. 3, p. 545, 2023.